Analyst

Accepted Manuscript

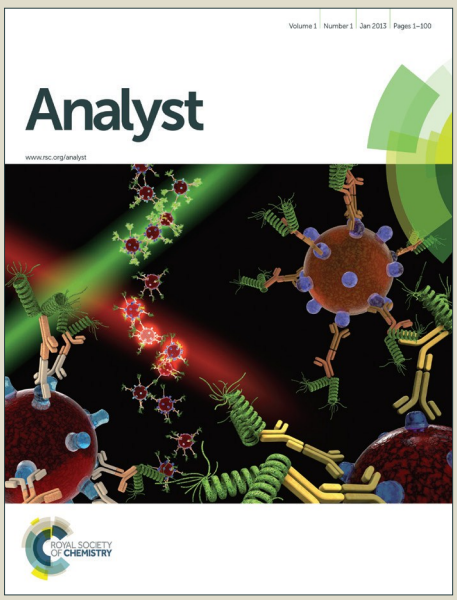

ROYAL SOCIETY OF CHEMISTRY

www.rsc.org/analyst

Journal Name

Cite this: DOI: 10.1039/c0xx00000x

www.rsc.org/xxxxxx

ARTICLE TYPE

Nicking Endonuclease-assisted signal amplification of split molecular aptamer beacon for biomolecules detection using graphene oxide as sensing platform

Xiang Li,[a] Xuelian Ding,[b] and Jing Fan[a]*

Received (in XXX, XXX) Xth XXXXXXXXX 200X, Accepted Xth XXXXXXXXX 200X
DOI: 10.1039/b000000x

Sensitive and selective detection of ultralow concentration of specific biomolecules is important in early clinical diagnoses and biomedical application. Many types of aptasensor have been developed for the detection of various biomolecules, but usually suffer from false positive signal and high background. In this work, we have developed an amplified fluorescence aptasensor platform for ultrasensitive biomolecules detection based on enzyme-assisted target-recycling signal amplification and graphene oxide. By using split molecular aptamer beacon and nicking enzyme, the typical problem of false positive signal can be effectively resolved. Only in the presence of target biomolecular, the sensor system is able to generate the positive signal, which significantly improves the selectivity of the aptasensor. Moreover, using graphene oxide as the super-quencher can effectively reduce the high background signal of sensing platform. We select vascular endothelial growth factor (VEGF) and adenosine triphosphate (ATP) as model analytes in the current proof-of-concept experiments. It is shown that under optimized conditions, our strategy exhibits high sensitivity and selectivity for the quantification of VEGF and ATP with low detection limit (1 pM and 4 nM, respectively). In addition, this biosensor has been successfully utilized in the analysis of real biological samples.

Intuoduction

Detection of biomolecules is of great significance in molecular diagnostics, clinical diagnoses and biomedical application, since the presence of abnormal concentrations of certain biomolecules (such as nucleic acids, proteins and some small molecules) inside the human body can reflect the human's health.[1] At present, the conventional methods, such as high performance liquid chromatography, mass spectrometry and luciferase-mediated bioluminescence have been widely used in the detection of biomolecules. However, the costly apparatus and complicated pretreatment procedures limited their use for on-site and real-time analysis. Thus seeking for simple, sensitive and selective methods for accurate detection of trace amounts of such biomolecules have raised to a great challenge in recent years.

Over the past decades, aptamers become powerful and extensively used tools for biomolecules analysis.[2] Compared with the conventional binding pair of antigen and antibody, aptamers offer several advantages, such as simple synthesis, good stability, design flexibility and wide applicability. This makes them promising ligands for bioanalytical applications. In particular, based on conformation change upon target binding, aptamers have been popularly employed in the development of novel assay methods for the detection of small molecules, metal ions and proteins by using various signal-transduction approaches such as electrochemistry, colorimetry, fluorescence, and so on.[3] Among these approaches, fluorescence aptasensors are particularly interesting due to their high stability, sensitivity, and feasibility of quantification. An attractive kind of fluorescence aptasensors is the molecular aptamer beacons (MABs), which holds the advantages of both the generality of an aptamer and the good signal transduction capability of molecular beacon (MB). During the past few years, traditional MABs have been used as effective tools for a wide range of applications.[4] While these strategies have their distinct advantages, there remain some challenging problems such as high background signal and low sensitivity. Therefore, it is important to find new approaches that can resolve these problems.

In order to reduce the background signal of sensor system and therefore to improve the sensitivity of fluorescence aptasensors, nanomaterials such as gold nanoparticles (AuNPs),[5] single-walled carbon nanotubes (SWNTs)[6] and graphene oxide (GO)[7] have been used as "super-quencher" to replace traditional organic quenchers. Nevertheless, the sensitivity is strictly limited owing to the 1:1 hybridization ratio, which means that one aptamer can bind with only one target molecule.

To overcome this shortcoming, signal amplification with target recycling strategy has been utilized to increase the sensitivity of aptamer-based assays in a series of recent studies.[8] Toward this end, DNA enzymes have been employed in the target recycling-oriented amplification assays for sensitive detection of biomolecules. For instance, DNase I and Exo III have been popularly used to recycle the analyte-substrate through the biocatalytic ''digestion'' of the aptamer component of the aptamer-substrate complex. However, recent research demonstrates that the aptamer probe may be digested by DNase I

or Exo III in the absence of target as well, which causes high background noise and false positive signal at low concentration of target.[9] In order to resolve these problems, nicking enzyme has attracted considerable efforts due to their excellent capability in mediating signal amplification in recent years. Nicking endonucleases are a special family of restriction endonucleases, which can recognize specific nucleotide sequences in double strand DNA and catalyze the cleavages of only one strand of double strand DNA at the fixed position relative to the recognition sequence. Some novel fluorescence biosensors based on nicking enzyme-assisted amplification strategy have been successfully applied for the highly sensitive detection of nucleic acids,[10] metal ions,[11] proteins[12] and some small molecules[13]. Nevertheless, most of the nicking enzyme based biosensors use Taqman probes or molecular beacon as signaling DNA probes to transduce optical signal, which needs to be double-labeled by a fluorophore and a quencher at the two opposite ends, resulting in high background signal and expensive operations. To the best of our knowledge, such nicking enzyme-assisted signal amplification systems have not been reported in any attempts for their use in the single labeled molecular aptamer beacon system.

In this work, we developed a fluorescence amplification assay strategy for the detection of biomolecules by using single labeled molecular aptamer beacon as the recognition element, in which GO was used as a super fluorescence quencher to reduce background signal-noise, and nicking enzyme was used as catalyst to realize enzyme-catalyzed target-recycling signal amplification. Compared with traditional homogeneous aptasensors, our strategy offers several significant advantages. First, the GO-based molecular aptamer beacon sensor has low background signal as compared to the conventional dually labeled fluorescent molecular aptamer beacon sensors due to the super quenching ability of GO. Second, in contrast to the double-labeled molecular beacon, the probe is only labeled with a single dye, which reduces the cost for analyst detection. Additionally, using nicking enzyme as an amplifying biocatalyst can improve the versatility and sensitivity of the aptasensor assays. In addition, the specific cleavage ability of the nicking enzyme requires a completely matched target and, thus the selectivity of the strategy is highly improved. From these advantages, we expect that this strategy may be a generalized platform for biomolecules detection.

Materials and methods

Regents and material

All oligonucleotides used in this work were synthesized and HPLC-purified by Shanghai Sangon Biotechnology Co., Ltd. (Shanghai, China). The sequences of all oligonucleotides (Apt 0, Apt 1, Apt 2, Apt 3 and Apt 4) were listed in Table S1. Recombinant human $VEGF_{165}$ was purchased from PeproTech Inc (Rocky Hill, USA). Thrombin, human serum albumin, immunoglobulin G, lactic acid, glucose, adenosine triphosphate (ATP), guanidine triphosphate (GTP), cytosine triphosphate (CTP) and uridine triphosphate (UTP) were purchased from Shanghai Sangon Biotech. Co., Ltd. (Shanghai, China). The nicking endonuclease, Nt.CviPII, and 10×NEBuffer 2 (500 mM NaCl, 100 mM Tris-HCl, 100 mM $MgCl_2$, and 10 mM dithiothreitol, pH 7.9) were purchased from New England BioLabs Ltd. (Beijing, China). Graphene oxide was synthesized from natural graphitic powder according to Hummer's method, which was reported in our previous work.[14] All other reagents were analytical grade and used without further purification. Doubly distilled water was used throughout the work. All stock solutions were stored in the dark at 0-4℃.

Apparatus

All fluorescence spectra were obtained using a Cary Eclipse fluorescence spectrophotometer (Varian, America). The excitation wavelength was λ =495 nm and the fluorescence measurements were carried out at 37℃ using a single cell peltier accessory to control temperature.

Assay Procedures

In a typical experiment, various amounts of $VEGF_{165}$ were incubated at 37℃ in 495 μL 1×NEBuffer 2 solutions containing 20 nM Apt 1, 20 nM Apt 2 and 0.25 U/μL Nt.CviPII for 50 min. Then 5 μL of GO (1.5 mg/mL) was added to the mixture and the fluorescence measurement was carried out after 5 min of the GO addition. The fluorescence intensity was measured at 520 nm. For ATP detection, various amounts of ATP were incubated at 37℃ for 90 min in 490 μL 1×NEBuffer 2 solutions containing 100 nM Apt 3 and 100 nM Apt 4 and 0.5 U/μL Nt.CviPII. Then 10 μL of GO (2.5 mg/mL) was added to the mixture and the fluorescence measurement was carried out after 5 min of the GO addition. The fluorescence intensity was measured at 520 nm.

Preparation of the real biological samples

For the determination of ATP in real biological samples, the fresh liver samples of healthy rats (provided by Sanquan Medical College, Xinxiang Medical University) were prepared. Briefly, the rat liver tissue was quickly mixed with 3 mL of $HClO_4$ (0.4 M) in ice cooled mortar. After grinding 20 min, the mixture was centrifuged at 10000 rpm for 10 min at 4℃ and the upper supernatant solution was collected. Then, 5 mol/L KOH was used to adjust the pH to 7.0. Finally, the above mixture was centrifuged at 10000 rpm for 5 min at 4℃ again and the upper supernatant solution was collected for further detection. For our proposed nicking enzyme-assisted signal amplified fluorescence strategy, the collected samples were diluted 100-fold with 1×NEBuffer 2 and then immediately used for ATP detection. The detection process of ATP in real biological sample was the same as in the buffer solution.

Results and discussion

The working principle of fluorescence amplification assay for the detection of biomolecules was illustrated in scheme 1. The aptamer was splitted into two subunits (Apt 1 and Apt 2). Apt 1 was designed as a molecular beacon structure, which has the specific loop sequence (containing 20 bases) for target binding and also contains the cleavage site for the nicking endonuclease,

while Apt 2 was designed as a single strand oligomer (containing 20 bases), which has not been labeled with any dye molecule. In the absence of a target, these two subunits did not hybridize with each other to form a stable complex due to the mismatched base pairs. The introduction of GO to the FAM-labeled Apt 1 and Apt 2 solution would result in strong binding between nucleotide bases and aromatic structure of GO via π-stacking, bringing the fluorophore into close proximity with the GO surface. Consequently, the fluorescence of FAM was quenched via energy transfer from dye to GO. However, in the presence of a target, the target and Apt 2 could hybridize cooperatively with the loop of Apt 1 to open the hairpin of Apt 1, thus forming the target/aptamer complex with a duplex DNA region. In this target/aptamer complex, there was full recognition site for nicking endonuclease. Then the nicking endonuclease could bind to this complex and cleave the recognition site. After nicking, the FAM-labeled Apt 1 was cleaved into two short DNA fragments (one contains 8 bases, the other contains 22 bases). The introduction of GO into the sensing solution could result in weak quenching of the fluorescence of FAM due to the weak affinity of the short FAM-labeled oligonuleotide fragment to GO, and the fluorescence intensity would gradually increase. In addition, the target and Atp 2 released by the nicking endonuclease-catalyzed cleavage of the target/aptamer complex could hybridize with another FAM-labeled Apt 1 probe to initiate the second cycle. Once the nicking enzyme cleavage process was triggered, continuous enzyme cleavage of the FAM-labeled Atp1 probe would take place. Finally, each target could go through many cycles, leading to a substantial increase of the fluorescence intensity and thus signal amplification. Because two splitted aptamers lack secondary structures, this split molecular aptamer beacon does not yield false positive or nonspecific signals compared with traditional liner aptasensors. To obtain a positive signal, both parts of the splitting aptamer must be in the proximity of each other, which only occurs when the probe bound to the target.[15]

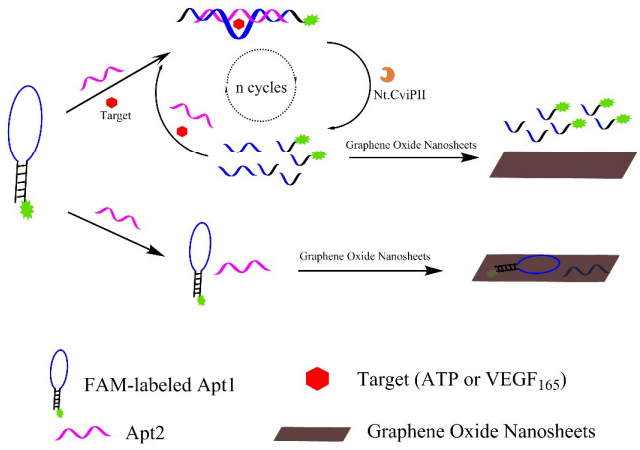

Scheme 1 Schematic illustration of the assay for the detection of biomolecules.

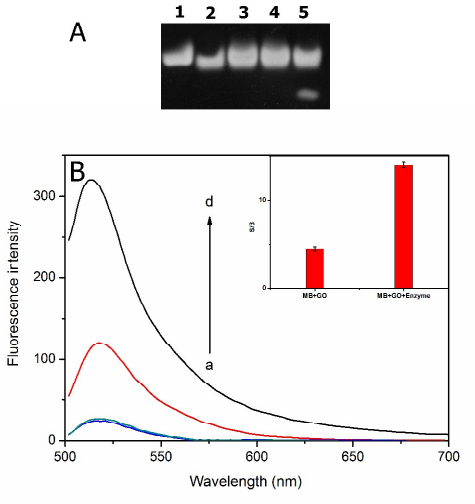

Fig. 1 (A) Native PAGE analysis of the sensing system. Lane 1, Apt 1 alone; lane 2, Apt 2 alone; lane 3, Apt1+Apt2; lane 4, Apt1+Apt2+Nt.CviPII;lane 5, Apt1+Apt2+Nt.CviPII+$VEGF_{165}$. All samples were monitored by using non-denaturing 15% polyacrylamide gel electrophoresis in 1× TBE at 70 V for 90 min. The gel was recorded by Tanon GIS-1000 Gel Imaging System after being stained by ethidium bromide. (B) Fluorescence emission spectra of Apt 1+Apt 2 under different conditions in 1×NEBuffer 2: (a), Apt 1+Apt 2+GO; (b), Apt 1+Apt 2+Nt.CviPII+GO; (c), Apt 1+Apt 2+$VEGF_{165}$+GO; (d), Apt 1+Apt 2+$VEGF_{165}$+Nt.CviPII+GO. Inset is the signal-to-background ratio (S/B) of the Apt1+Apt2+GO system generated by 5 nM of $VEGF_{165}$ in the absence and presence of Nt.CviPII, respectively ([Apt 1] = [Apt 2] = 20 nM, [GO] = 10 μg/mL, [$VEGF_{165}$] = 5 nM, and [Nt.CviPII] = 0.2 U/μL).

To demonstrate the feasibility of our enzyme-assisted target recycling signal amplification strategy, vascular endothelial growth factor (VEGF) was chosen as the model target which is a key regulator of both physiologic and pathologic angiogenesis, and can stimulate vascular endothelial cell growth, survival, and proliferation.[16] The signaling protein VEGF in serum samples was identified as the potential biomarker for a number of human diseases, such as cancer, rheumatoid arthritis, and psoriasis and proliferating retinopathy. Therefore, a rapid and convenient method for VEGF detection with high sensitivity and selectivity is in great demand. It is known that VEGF has several isoforms that contain various numbers of residues as a result of selective splicing. As the most abundantly expressed isoform, $VEGF_{165}$ plays a vital role in angiogenesis. Thus, we selected $VEGF_{165}$ as the analyte in this study. According to the literature,[17] the anti-$VEGF_{165}$ DNA aptamer, which adapts a G-quadruplex configuration, was splitted into two oligomers (Apt 1 and Apt 2). The designed Apt 1 has a hairpin structure with a sequence of 5'-GCA GCT ATG TGG GGG TGG ACG T↓***CC A***GC TGC-FAM-3'. The underlined portion is the loop region, which is designed as a subunit for the recognition of $VEGF_{165}$. The complementary stem portions are at the two ends of the loop region. The sequence in italic bold is the recognition domains of endonucleases, and the arrow indicates the nicking position. On

the other hand, Apt 2 was designed as another subunit for the recognition of $VEGF_{165}$, which has the sequence of 5'-TGG ATA CGG CCG GGT AGA TA-3'. The nicking endonuclease used in this work is Nt.CviPII (New England Biolabs), which recognizes double-stranded DNA (dsDNA) and only cleaves the single strand DNA on the 5' side of the recognition site (5'-(cut)CCX-3' , X = A, G, or T). Firstly, the native polyacrylamide gel electrophoresis was performed to validate the experimental feasibility. As shown in Fig. 1A, we can see bright bands for Apt 1 (lane 1) and Apt 2 (lane 2), respectively. In the absence of target, no new product band was obtained regardless of the absence or presence of Nt.CviPII (see lanes 3 and 4). However, a new product band (cleaved Apt 1 probe) appeared in land 5, which was only generated in the presence of the target. These results are in agreement with those shown in scheme 1, demonstrating the feasibility of our sensing protocol.

The target-induced fluorescence changes in the presence and absence of Nt.CviPII were also investigated to verify the feasibility of the designed amplified strategy for $VEGF_{165}$ detection. As shown in Fig. 1B, in the absence of $VEGF_{165}$, the fluorescence of Apt 1+Apt 2 was almost entirely quenched by GO regardless of the presence or absence of Nt.CviPII (curves a, and b). This indicates strong adsorption of Apt 1+Apt 2 on GO surface and high fluorescence quenching efficiency of GO. In the absence of $VEGF_{165}$, the Nt.CviPII cannot interact with the aptamer probe to induce the increase of fluorescence. Meanwhile, upon the addition of $VEGF_{165}$, the fluorescence signal of Apt 1+Apt 2-GO was partially recovered with a signal-to-background ratio of 4.5 (curve c), which suggests that the $VEGF_{165}$ may bind with Apt 1+Apt 2 to form the $VEGF_{165}$/aptamer complex, and the complex leaves the GO surface to induce the recovered fluorescence. However, during the incubation of the Apt 1+Apt 2 probe with $VEGF_{165}$ and Nt.CviPII, the fluorescence intensity exhibited significant restoration with a signal-to-background ratio of 13.6 (curve d). This is an indicative of the fact that Nt.CviPII can catalyze the cleavage of $VEGF_{165}$/aptamer complex formed from $VEGF_{165}$ binding with Apt 1+Apt 2 to achieve the target-recycling signal amplification. Additionally, we prepared double-labeled molecular aptamer beacon (DMAB) for the detection of $VEGF_{165}$ (see scheme S1). It can be seen from Fig. S1 that after adding $VEGF_{165}$ in the solution of traditional DMAB, the fluorescence intensity was slightly recovered with a signal-to-background ratio of 1.05. These results clearly indicate that the introduction of Nt.CviPII to sensor system significantly improves sensitivity since they greatly realize the target-recycle signal amplification.

In order to achieve the best assay performance, we optimized the amplification sensing conditions including the concentration of GO, the amount of Nt.CviPII and the nicking-cleavage reaction time. It was fond that GO concentration was one of critical factors in the detection system. When the GO concentration was too low, the background signal was rather high, possibly due to the incomplete quenching of GO on the fluorescence of FAM-labeled Apt 1 probe. However, when the GO concentration was too high, excess amount of GO could also quench the fluorescence of cleavage-produced short FAM-DNA fragments. Thus, it was necessary to optimize the amount of GO to give the highest fluorescence enhancement. As shown in Fig. 2A, the fluorescence intensity ratio (F/F_0, where F_0 and F were the fluorescence intensity in the absence and the presence of $VEGF_{165}$, respectively) of the sensing system increased significantly when the concentrations of GO increased from 0 to 15 μg/mL. As the concentration of GO was higher than 15 μg/mL, the F/F_0 decreased with a further increase of GO concentration, which might be ascribed to the excessive quenching effect of GO at a high concentration on the cleavage-produced short FAM-DNA fragments. Therefore, 15 μg/mL GO was chosen as the optimal concentration in the next experiments.

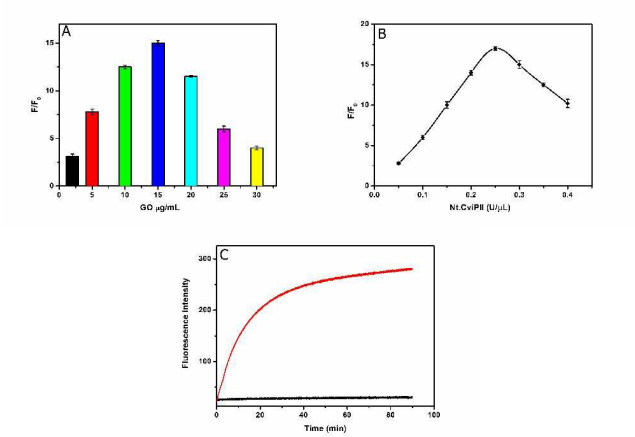

Fig. 2 (A) The effect of GO concentration on the fluorescence response of the sensing system, where F_0 and F are the fluorescence intensity in the absence and presence of $VEGF_{165}$, respectively ([Apt 1] = [Apt 2] = 20 nM, [$VEGF_{165}$] = 5 nM, [Nt.CviPII]= 0.2 U/μL); (B) The effect of Nt.CviPII concentration on the fluorescence response of the sensing system ([Apt 1] = [Apt 2] = 20 nM, [$VEGF_{165}$] = 5 nM, [GO]= 15 μg/mL); (C) Time-dependent fluorescence intensity of the sensor system with and without $VEGF_{165}$ ([Apt 1] = [Apt 2] = 20 nM, [$VEGF_{165}$] = 5 nM, [GO]= 15 μg/mL, [Nt.CviPII]= 0.25 U/μL). The error bar was calculated from three independent experiments.

It was also found that the amount of Nt.CviPII could influence the sensitivity of aptasensor. Low concentration of enzyme might result in a longer period of enzymatic catalytic reaction and no obvious signal amplification, whereas high concentrations of enzyme would lead to non-specific nicking recognition site cleavage and increase of background signal. Thus, the effect of concentration of Nt.CviPII was further studied and the results were shown in Fig. 2B. It was clear that the F/F_0 of the sensing system increased with increasing Nt.CviPII concentration up to 0.25 U/μL. However, at the concentration higher than 0.25 U/μL, the F/F_0 of the sensing system decreased rapidly. Taking into account the response sensitivity, 0.25 U/μL of Nt.CviPII was used in the final solution.

The enzyme cleavage time was also an important factor for sensing systems. In order to obtain optimal assay time, the fluorescence intensity of Apt 1+Apt 2-GO system incubated with nicking enzyme for different enzyme cleavage time were measured in the presence and absence of $VEGF_{165}$, respectively. As shown in Fig. 2C, in the presence of $VEGF_{165}$, the fluorescence intensity increased when the reaction time was prolonged (the red line). The rapid increase in fluorescence intensity clearly demonstrates that the designed nicking enzyme-

assisted target recycling was indeed taking place. However, in the absence of $VEGF_{165}$, fluorescence intensity of the solution remained virtually unchanged under the same experimental conditions (the black line). This suggests that in the absence of $VEGF_{165}$, Nt.CviPII cannot catalyze the cleavage of Apt 1 to induce the fluorescence enhancement. Taking both the effectiveness and the reaction rate into consideration, we chose 50 min as the nicking enzyme reaction time for our reactions.

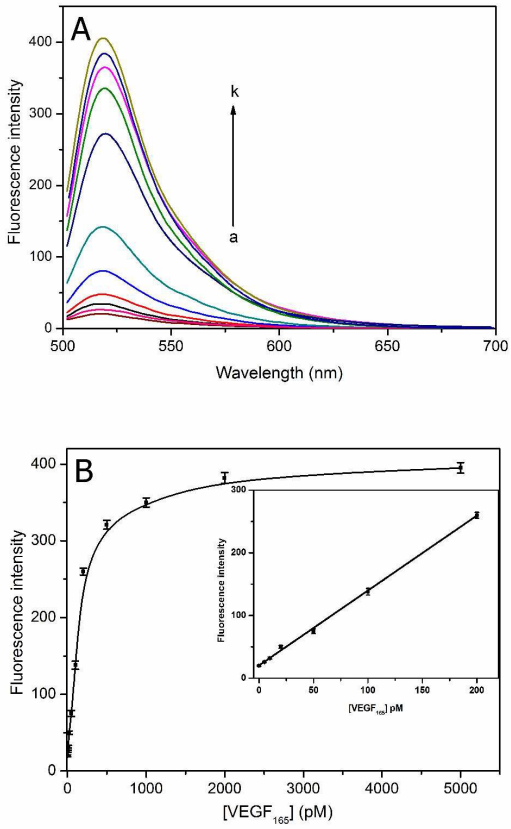

Fig. 3 (A) Fluorescence emission spectra of the Apt1+Apt2-GO system after incubation with Nt.CviPII and different concentrations of $VEGF_{165}$: (a-k), 0, 5, 10, 20, 50, 100, 200, 500, 1000, 2000 and 5000 pM; (B) The relationship between the fluorescence intensity and the concentration of $VEGF_{165}$. The inset shows the linear relationship in the concentration rang from 5 to 200 pM. The error bar was calculated from three independent experiments.

Based on the above results, 15 μg/mL of GO, 50 min of reaction time and 0.25 U/μL of Nt.CviPII were selected for the further $VEGF_{165}$ sensing experiments. Under the optimal conditions, we investigated the fluorescence spectra of the sensing system incubated with different concentrations of $VEGF_{165}$. As illustrated in Fig. 3A, a dramatic increase in the fluorescence intensity was observed with increasing concentrations of $VEGF_{165}$. By measuring the fluorescence intensity of the solution upon addition of different concentrations of $VEGF_{165}$, we obtained the working curve for $VEGF_{165}$ concentration ranging from 5 to 5000 pM (Fig. 3B). The inset in Fig. 3B revealed a linear response to the concentration of $VEGF_{165}$ over the range of 5-200 pM (R=0.9971). The detection limit was 1 pM based on 3σ. A control experiment without Nt.CviPII was carried out to confirm if the efficient Nt.CviPII-assisted target recycling signal amplification contributes to the high sensitivity of the approach. In doing so, Apt 1+Apt 2+GO system at different concentrations of $VEGF_{165}$ was performed in the absence of Nt.CviPII. It can be seen from Fig. S2 that the limit of detection was 200 pM and no signal amplification was observed. Thus, we can conclude that it is the Nt.CviPII-assisted target recycling signal amplification that lowers the limit of detection by two orders of magnitude for the detection of $VEGF_{165}$. In comparison with other DNA-based fluorescence sensors for $VEGF_{165}$ (Table S2), Nt.CviPII- assisted target recycling sensor shows a lower detection limit than most of the previously reported DNA-based fluorescence sensors for $VEGF_{165}$ although this sensor system makes the process somewhat complicated. The enhanced sensitivity might be attributed to the low background noise by GO and the signal amplification by Nt.CviPII -assisted target recycling.

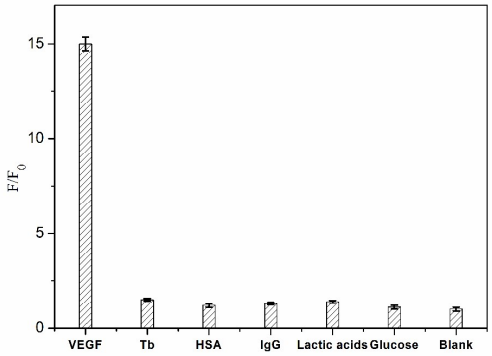

Fig. 4 Selectivity of the sensing system for $VEGF_{165}$ over other common biomolecules: the concentrations of biomolecules were: 5 nM of $VEGF_{165}$, 10 μM of thrombin (Tb), human serum albumin (HSA), immunoglobulin G (IgG), lactic acids or glucose, respectively. The error bar was calculated from three independent experiments.

To evaluate the specificity of the fabricated biosensor for $VEGF_{165}$, we exposed the system to other biomolecules such as thrombin (Tb), human serum albumin (HSA), immunoglobulin G (IgG), lactic acid and glucose under the same experimental conditions as those for $VEGF_{165}$. As shown in Fig. 4, significant fluorescence signal enhancement was observed in the presence of $VEGF_{165}$, whereas the fluorescence intensities remained low for the other tested analytes even though their concentrations were 2000 times higher than $VEGF_{165}$. These results demonstrated good selectivity of the assay for $VEGF_{165}$, which was probably resulted from the specific and high affinity binding of the aptamer to the target and the subsequent enzyme cleavage process induced by the binding events.

To examine if our signal amplification strategy can be applied to the detection of other molecules by using particular aptamers, we further designed Nt.CviPII-assisted target recycling signal amplification method for the detection of adenosine triphosphate (ATP). As a major cellular energy currency, ATP plays a critical role in various cellular metabolic functions and biochemical

pathways in cell physiology.[18] It was reported that abnormal concentration of ATP may be tightly associated with cardiovascular, Parkinson's and Alzheimer's diseases.[19] ATP has also been widely used as an indicator for cell viability and cell injury. Therefore, routine detection of ATP is of highly importance in clinical diagnoses. According to the literature,[6b] the ATP aptamer could be split into two oligomers (Apt 3 and Apt 4). The designed Apt 3 has a hairpin structure with a sequence of 5'-CGA CGA CCT GGG GGA GTA T↓***CC G***CG TCG-FAM -3', while Apt 4 has a sequence of 5'-CGG AGC GGA GGA AGG T-3'. Similarly, the assay conditions were optimized to obtain the best performance of the sensing system. It was shown that using 50 μg/mL of GO and 0.5 U/μL of Nt.CviPII with incubation time of 90 min for nicking-cleavage reaction could provide maximum S/N ratio for the sensing system (see ESI, Fig. S3-5). Fig. 5 illustrates the fluorescence spectra upon addition of different concentrations of ATP, and the fluorescence intensity change shows a linear relationship with the concentration of ATP over the range of 0.01-1 μM (R = 0.9976). A detection limit of 4 nM for ATP was estimated based on 3σ. This detection limit is about three orders of magnitude higher than that of traditional homogeneous aptasensors, and is comparable to or better than that of other reported amplified aptasensors (Table S3).

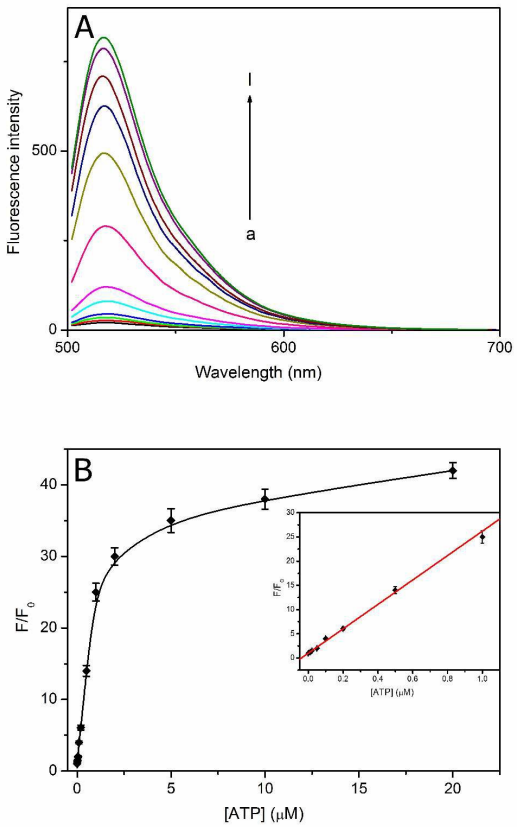

Fig. 5 (A) Typical fluorescence spectra of Apt 3+Apt 4-GO upon the addition of Nt.CviPII and ATP at different concentrations: (a-l), 0, 0.01, 0.02, 0.05, 0.1, 0.2, 0.5, 1, 2, 5, 10 and 20 μ M; (B) Calibration curve for ATP detection: inset, magnification of the plot in the range from 0.01 to 1 μ M; [Apt 1] = [Apt2] = 100 nM, [GO] = 50 μg/mL, [Nt.CviPII] = 0.5 U/μL.

To test the specificity of the assay for ATP detection, we selected four ATP analogues (ATP, GTP, CTP and UTP) to perform the control experiments. As shown in Fig. S6, among these analytes, only ATP resulted in a significant increase in the fluorescence intensity, while control molecules did not lead to any discernible fluorescence change, indicating that our sensing system exhibits an excellent selectivity to ATP over other competing analytes.

Table 1 Comparisons of this amplified method with the traditional HPLC Method for the detection of ATP in the freshly rate liver extractions

Sample	This method (μ M)[a]	RSD (%, n=3)	HPLC (μ M)[a]	RSD (%, n=3)
1	11.23	3.2	11.40	3.5
2	12.13	3.8	12.03	3.6
3	12.20	3.5	12.32	3.7

[a] Each sample was analyzed in triplicate, and the results were the average values

To examine the feasibility of our approach in complex biological matrixes, the determination of ATP in three healthy rats liver cell extractions were performed. As shown in Table 1, the detection results of ATP in diluted cell extractions by the amplified aptasensor were in reasonable agreement with those obtained by HPLC method, which indicates that the sensing approach developed in the present work can be applied for the detection of ATP in real biological samples.

Conclusions

In summary, we have developed a general fluorescence method based on graphene oxide, cyclic enzymatic signal amplification, and molecular aptamer beacon probe for highly efficient detection of biomolecules, such as $VEGF_{165}$ and ATP. This approach shows advantages such as high sensitivity, excellent specificity and simplicity. Combining the low back-ground signal and nicking enzyme-assisted signal amplification, the developed strategy has a detection limit of 1 pM and 4 nM for $VEGF_{165}$ and ATP, respectively, which are much lower than the previously reported fluorescence biosensors. This sensitivity is about 3 orders of magnitude higher than that of homogeneous aptasensors without amplification. By taking advantage of the highly binding specific between aptamers and targets, the developed aptasensor shows significantly high selectivity toward target ($VEGF_{165}$ or ATP) and can distinguish the target biological small molecules from their analogues. Moreover, the proposed method is capable of detecting target in complicated biological samples such as cell extractions. Therefore, by changing the corresponding aptamer, it is expected that this simple and highly sensitive strategy would have important applications in a wide range of areas, such as biological, medical diagnostics and environmental monitoring.

Acknowledgements

This work was supported by the National Natural Science Foundation of China (21377036) and Postdoctoral Research Sponsorship in Henan Province (Grant No. 2014064).

Notes and references

[a] *School of Environment, Henan Key Laboratory for Environmental Pollution Control, Key Laboratory for Yellow River and Huai River Water Environment and Pollution Control, Ministry of Education, Henan Normal University, Xinxiang, Henan 453007, P. R. China*

[b] *Department of Chemistry, Sanquan Medical College, Xinxiang Medical University, Xinxiang, Henan 453003, P. R. China*

**Address correspondence to Jing Fan, School of Environment, Henan Normal University, Xinxiang, Henan 453007, P. R. China. Tel: +86-373-3325719. E-mail: fanjing@htu.cn*

† Electronic Supplementary Information (ESI) available: the oligonucleotides used, comparison of fluorescence methods for determination of VEGF165, Sensing platforms for the detection of ATP, Scheme S1 and Figure S1-S6. See DOI: 10.1039/b000000x/

1 (a) E. Hendry, T. Carpy, J. Johnston, M. Popland, R. V. Mikhaylovskiy, A. J. Lapthorn, S. M. Kelly, L. D. Barron, N. Gadegaard, M. Kadodwala, *Nat. Nanotechnol.*, 2010, **5,** 783-787; (b) S. P. Song, Y. Qin, Y. He, Q. Huang, C. H. Fan, H. Y. Chen, *Chem. Soc. Rev.,* 2010**,** **39,** 4234-4243.

2 (a) E. J. Cho, J. W. Lee, A. D. Ellington, *Ann. Rev. Anal. Chem.,* 2009, **2,** 241-264; (b) J. W. Shen, Y. B. Li, H. S. Gu, F. Xia, X. L. Zuo, *Chem. Rev.,* 2014, **114,** 7631-7677; (c) W. H. Tan, M. J. Donovan, J. H. Jiang, *Chem. Rev.,* 2013, **113,** 2842-2862; (d) H. Q. Zhang, F. Li, B. Dever, X. F. Li, X. C. Le, *Chem. Rev.,* 2013, **113,** 2812-2841; (e) W. W. Zhao, J. J. Xu, H. Y. Chen, *Chem. Rev.,* 2014, **114,** 7421-7441.

3 (a) B. R. Baker, R. Y. Lai, M. S. Wood, E. H. Doctor, A. J. Heeger, K. W. Plaxco, *J. Am. Chem. Soc.,* 2006, **128,** 3138-3139; (b) Y. Du, S. J. Guo, H. X. Qin, S. J. Dong, E. K. Wang, *Chem. Commun.,* 2012, **48,** 799-801; (c) L. Wu, X. H. Zhang, W., Liu, E. H. Xiong, J. H. Chen, *Anal. Chem.,* 2013, **85,** 8397-8402; (d) F. Xia, X. L. Zuo, R. H. Yang, Y. Xiao, et al. *Proc. Natl. Acad. Sci. USA,* 2010, **107,** 10834-10841; (e) Y. Xu, G. F. Cheng, P. G. He, Y. Z. Fang, *Electroanaly.* 2009, **21,** 1251-1259.

4 (a) X. Fang, A. Sen, M. Vicens, W. H. Tan, *ChemBioChem,* 2003, **4,** 829-834; (b) M. N. Stojanovic, P. Prada, D. W. Landry, *J. Am. Chem. Soc.,* 2001, **123,** 4928-4931; (c) Z. Y. Xiao, X. T. Guo, L. S. Ling, *Chem. Commun.,* 2013, **49,** 3573-3575.

5 (a) B. Dubertret, M. Calame, A. J. Libchaber, *Nat. Biotechnol.,* 2001, **19,** 365-370; (b) D. J. Maxwell, J. R. Taylor, S. Nie, *J. Am. Chem. Soc.,* 2002. **124,** 9606-9612; (c) J. Zhang, L. Wang, H. Zhang, F. Boey, S. P. Song, C. H. Fan, *Small,* 2010, **6,** 201-204.

6 (a) L. A. Yan, H. Shi, X. X. He, K. M. Wang, J. L. Tang, M. Chen, X. S. Ye , F. Z. Xu, Y. L. Lei, *Anal. Chem.,* 2014, **86,** 9271-9277; (b) S. J. Zhen, L. Q. Chen, S. J. Xiao, Y. F. Li, P. P. Hu, L. Zhan, L. Peng, E. Q. Song, C. Z. Huang, *Anal. Chem.* 2010, **82,** 8432-8437.

7 (a) H. Chang, L. Tang, Y. Wang, J. Jiang, J. H. Li, *Anal. Chem.,* 2010, **82,** 2341-2346; (b) H. Dong, W. Gao, F. Yan, H. Ji, H. X. Ju, *Anal. Chem.,* 2010, **82,** 5511-5517; (c) Y. Zhang, Y. Liu, S. J. Zhen, C. Z. Huang, *Chem. Commun.,* 2011, **47,** 11718-11720.

8 (a) J.P. Lei and H.X. Ju, Chem. Soc. Rev., 2012, **41**, 2122-2134; (b) Y.V. Gerasimova and D. M. Kolpashchikova, Chem. Soc. Rev., 2014, **43,** 6405-6438; (c) X.T. Shen, M.H. Zhang, S.Y. Niu and C. Shi, Analyst, 2015, **140**, 6489-6492; (d) S.J. Ye, Y.Y. Guo, J. Xiao and S.S. Zhang, Chem. Commun., 2013, **49**, 3643-3645; (e) J. L. He, Z. S. Wu, H. Zhou, H. Q. Wang, J. H. Jiang, G. L. Shen and R. Q. Yu, Anal. Chem., 2010, 82, 1358–1364.

9 (a) X.Y. Lin, L. Cui, Y. S. Huang, Y. Lin, Y. Xie, Z. Zhu, B. C. Yin, X. Chen, C. Y. Yang, *Chem. Commun.,* 2014, **50,** 7646-7648; (b) X. Q. Liu, R. Freeman, I. Willner, *Chem. Eur. J.* 2012, **18,** 2207-2211; (c) C. H. Lu, J. Li, M. H. Lin, Y. W. Wang, H. H. Yang, X. Chen, G. N. Chen, *Angew. Chem. Int. Ed.,* 2010, **49,** 8454-8457; (d) D. P. Tang, J. Tang, Q. F. Li, B. L. Su, G. N. Chen, *Anal. Chem.,* 2011, **83,** 7255-7259; (e) F. Xuan, X. T. Luo, I. M. Hsing, *Anal. Chem.,* 2013, **85,** 4586-4593.

10 (a) Y. Song, W. K. Li, Y. F. Duan, Z. J. Li, L. Deng, *Biosens. Bioelectron.* 2014, **55.** 400-404; (b) B. J. Zou, Y. J. Ma, H. P. Wu, G. H. Zhou, *Angew. Chem. Int. Ed.* 2011, **50,** 7395-7398.

11 X. L. Zhu, J. Zhao, Y. Wu, Z. M. Shen, G. X. Li, *Anal. Chem.,* 2011, **83,** 4085-4089.

12 (a) Y. Y. Tan, Q. P. Guo, X. Y. Zhao, X. H. Yang, K. M. Wang, J. Huang, Y. Zhou, *Biosens. Bioelectron.,* 2014, **51,** 255-260; (b) L. Y. Xue, X. M. Zhou, D. Xing, *Anal. Chem.* 2012, **84,** 3507-3513; (c) A. X. Zheng, J. R. Wang, J. Li, X. R. Song, G. N. Chen, H. H.Yang, *Chem. Commun.,* 2012, **48,** 374-376.

13 (a) Y. Huang, X. Q. Liu, L. L. Zhang, K. Hu, S. L. Zhao, B. Z. Fang, Z. F. Chen, H. Liang, *Biosens. Bioelectron.,* 2015, **63,** 178-184; (b) C. H. Lu, F. Wang, I. Willner, *Chem. Sci.,* 2012, **3,** 2616–2622.

14 (a) X. Li. G. K. Wang. X. L. Ding, Y. H. Chen, Y. P. Gou, Y. Lu, *Phys. Chem. Chem. Phys.,* 2013, **15,** 12800-12804; (b) X. Li, X. L. Ding, G. K. Wang. R.P. Hou, Y. X. Zhou, Y. Lu, *Sci. Adv. Mater.* 2014, **6,** 1936-1942.

15 (a) F. Jin, Y. Lian, J. H. Li, J. Zheng, Y. P. Hu, J. H. Liu, J. Huang, R. H. Yang, *Anal. Chimica. Acta.* 2013, **799,** 44-50; (b) Y. F. Bai, F. Feng, L. Zhao, Z. Z. Chen, H. Y. Wang, Y. L. Duana, *Analyst,* 2014, **139**, 1843-1846.

16 (a) N. Ferrara *J. Mol. Med.* 1999, **77,** 527-543; (b) N. Ferrara, H. P. Gerber, J. LeCouter, *Nat. Med,* 2003, **9,** 669-676; (c) D. J. Hicklin, L. M. Ellis, *J. Clin. Oncol,* 2005, **23,** 1011-1027.

17 (a) R. Freeman, J. Girsh, A. F. Jou, J. A. Ho, T. Hug, J. Dernedde, I. Willner, *Anal. Chem.* 2012, **84,** 6192-6198; (b) Y. Nonaka, K. Sode, K. Ikebukuro, *Molecules* 2010, **15,** 215-225.

18 T. Pérez-Ruiz, V. Tomás, J. Martín, *Anal. Bioanal. Chem.* 2003, **377,** 189-194.

19 (a) S. Przedborski, M. Vila, *Clin. Neurosci. Res.,* 2001, **1,** 407-418; (b) H. Yokoshiki, M. Sunagawa, T. Seki, N. Sperelakis, *Am. J. Physiol. Cell Physiol,* 1998, **274,** 25-37.